

Appendix B

B1 Refraction data and their pre-processing

The first refraction arrivals along the whole S02 and S03 profiles and the northwestern part of the S04 profile were evaluated. Using the software ZPLOT (Zelt 1994), the refraction arrivals were picked in 37 shot gathers. Table B1 presents a visual five-degree quality assessment of the picked travel-times at single shot gathers: 1 stands for the best relative S/N ratio, 5 for the unusable records. Last column comprises the maximum offsets of reading. Except the S03 profile, the shot gathers displayed considerably variable S/N ratios. For the S04 shot gathers, the maximum offsets varied from 15 km to 250 km. The S02 and S03 first arrivals of the refraction waves were usually readable up to 100–150 km. Five S02 and S03 shot gathers even allowed reliable readings up to 200–300 km.

B2 Static corrections

The SUDETES 2003 profiles pass several mountainous ranges with the 800–1000 m altitudes descending to 160–70 m in the lowlands. The S04 shot-point/receiver heights vary from 780/825 m in the Krušné hory Mts. down to 245/158 m in the Elbe lowland, respectively (Fig. B1). The S02 and S03 lines pass still more extreme topography. They pass the Krkonoše or Orlické hory Mts. at ~1000 m asl and descend to 70 m asl in the lowland on the Polish territory. The static corrections are necessary to reduce the influence of the surface topography and the weathering layer on the travel times.

The static corrections were calculated for the fixed or floating reference level (RL) that substitutes the scatter of the receiver and shot-point altitudes (Fig. B1). For the S03 profile with a longer lowland part, the floating reference level was used. The uppermost velocities

were set to the near-surface velocities estimated at the shot points by means of the one-sided spline fits of the travel-time curves.

Three sets of corrections for each profile were calculated: the complete static corrections (DTRS) obtained as the sum of the partial receiver (DTR) and shot-point (DTS) corrections. Table B2 presents the maxima, minima and standard deviations characterizing each set. The DTRS standard deviations due to the S04, S02 and S03 profiles are 35, 68 and 35 ms, respectively. They may be considered as less important in comparison with other larger uncertainties occurring in input data. However, applying the static corrections, the extremes (up to ~200 ms in the shot-point altitudes, Tab. B2) were compensated which reduces large time shifts among the single travel-time curves. Their removal facilitates interpolation of the travel-times along the profile lines. The reference levels also properly define the upper boundaries of the output 2-D velocity models instead of the fuzzy 3-D scatters of the shot-point and station altitudes (see Fig. B1 and Tab. B1).

B3 Pre-processing of travel times for the 2-D inversion

As the first step of pre-processing, the complete DTRS static corrections were introduced. Figure B2 illustrates the original and pre-processed refraction arrivals used for the velocity determination along individual profiles. The close circles depict the static-corrected travel times $t(p_i, q_j)$ at their midpoint positions p , i.e. at the midpoint of the source–receiver distance q . The p -representation used in Fig. B2 is suitable for checking the travel-times in the reciprocal points – cf. the intersections of travel-time curves in Fig. B2. The midpoint (p variable) namely remains unchanged if the receiver and shot position are interchanged. A pair of the reciprocal travel-times then occupies a common midpoint position, and their discrepancy can easily be assessed and processed. The ray-based DRTG tomography uses the imaging rays with arbitrary emergence, i.e., not only at the original source–receiver positions.

To interpolate the input arrival times $t(p_i, q_j)$ for any p midpoint and q offset, a spline fitting governed by spline weights was used as follows.

First, all static-corrected travel-time curves (TTC) were re-sampled to a regular offset step $\Delta q = 2 \text{ km}$ (cross symbols in Fig. B2). The re-sampled travel times could then be arranged according to the increasing offsets, $2 \text{ km}, 4 \text{ km}, \dots$. In next step, the offset-dependent weights $w(q)$ were applied. They change the spline fit from the almost exact interpolation ($w=2$) to a slightly smoothing mode ($w=9$) set for the largest offsets. Using the offset-dependent spline fitting, the equal-offset travel times $t(p, q)$, $q=q_n$, were interpolated to the regular midpoint positions $p_m = 5, 10, \dots \text{ km}$. The chosen midpoint step $\Delta p = 5 \text{ km}$ is approximately six times lesser if compared to the average steps of shot-point deployments along the single profiles (Tab. B1). Figure B2 presents the regularly sampled time lines $t(p_m, q)$, $q=q_n$ obtained by the above pre-processing for all the S04, S02 and S03 profiles. The smoothing spline weights were chosen by trial and error so that the time lines $t(p, q)$, $q=const$, did not mutually intersect and simultaneously, the spline fit showed minimum RMS time deviations from the input static-corrected travel-times. The largest RMS deviations of the spline fits attained 60–80 ms at the 120 km offset. The time lines $t(p, q)$, $q=q_n$ are then monotonically increasing functions in the offset variable q for any fixed midpoint p_m . They represent the input data for the tomographic mapping. The equal-midpoint travel-time curves, $t(p, q)$, $p=p_m$, served to derive the initial 2-D velocity models for starting the DRTG iterations.

In conclusion, the applied static corrections reduce the influence of the surface topography and weathering layer. Using the spline fitting with the controlled smoothing mode allowed to obtain the input travel-times $t(p_m, q_n)$ rid of small-scale effects that are beyond the expected resolution. The useable part of the (p, t) input data domains is a trapezium-shaped so that it contains more than a half of imaging ray paths, i.e., their side boundaries just halved the

marginal ray path. Note that there are some blind ranges with no refraction data for small offsets at the beginning of the S02 and S03 profiles (Fig. B2). They signalize occurrences of low-velocity zones with no refraction returns.

B4 Input data errors

For the SUDETES 2003 profiles, Růžek et al. (2007) assessed the picking errors of about ~50 ms from the repeated shots at the same positions. However, for their 2-D models, the authors only required and attained the time fit of about 100 ms, i.e., twice more than the picking errors. Examine further sources of input errors and uncertainties.

Another source of input errors is the incompletely or no compensation of the surface topography and weathering layer, both considerably variable in velocities and thicknesses. The static corrections that were applied for the S04, S02 and S03 profiles reduce this influence. Their RMS 35, 68 and 35 ms (Tab. B2) could be viewed as the limits of the near-surface uncertainties for these profiles. A significant source of input uncertainties could also be the travel-time discrepancies detected at the reciprocal position. They occur in the S04, S02 and S03 original data – see the original travel-times curves near their mutual intersections in Fig. B2. They must be considered as input errors although the spline fitting applied for the time lines $t(p,q)$, $q=const$ balanced (and then removed) them in the midpoint positions (Fig. B2). The original reciprocal travel-time discrepancies namely still characterize adequacy of the 2-D simplification, which will be used for the inversion of the 3-D data. They then represent a further component of the input errors for our 2-D modeling. To estimate their RMS values, a wider set of near-reciprocal travel times must be analyzed. It contains the equal-offset travel times due to the different shot points but having near midpoints.

Figure B3 presents such near-reciprocal travel times selected from the S04, S02 and S03 data. The travel times whose midpoints mutually differ less than 6 km are involved. Because

of the used 2 km offset step, their scatters repeat in the 0–2 km, 2–4 km and 4–6 km intervals (Fig. B3). The scatters should perfectly repeat in the case of the laterally homogeneous media. At the presence of lateral inhomogeneities, they may somewhat differ. Evaluating their RMS values in the single intervals, their final RMS can then be extrapolated for the proper reciprocal positions at the zero-separation distance (closed squares in Fig. B3). The found trends then provided the σ_r reciprocal discrepancies of 117, 106 and 75 ms of the S04, S02 and S03 travel-times (dotted in Fig. B3).

Other error components stem from the used spline fitting of the equal-offset time lines and travel-times curves. The standard deviations of the spline fits increase with the offset and reach maximum values of 60–80 ms at the 120 km offset. Then, the found reciprocal errors of 117, 106 and 75 ms are still the most significant component of the analyzed time uncertainties. These values will be considered as the thresholds to which it is reasonable to constrain the single 2-D velocity models.

The picked travel-times have passed a number of operations. However, the smoothed time lines $t(p,q)$, $q=const$, rid of the reciprocal discrepancies, can be viewed as a maximum likelihood realization of the original input travel times adapted for 2-D inversion. In other words, additional measurements are supposed to confirm their course in the intermediate points. The time lines constrain the model rays emerging not only at the original source–receiver pairs but for their arbitrary emergence within the data range. The input data in Fig. B2 were, of course, prepared under many simplifying assumptions. However, the experience has shown that the velocity models, constrained in this way, exhibited a higher useful resolution than those fitting exclusively the travel times at the original source–receiver positions (Novotný 2013).

References

- GRAD M, ŠPIČÁK A, KELLER GR, GUTERCH A, BROŽ M, BRÜCKL E, HEGEDŮS E (2003) SUDETES 2003 seismic experiment. *Stud Geophys Geod* 47: 681–689
- NOVOTNÝ M (2013) Refraction Tomography of the Bohemian Massif structures: a critical review and reply to the comments of Hrubcová et al. *Surv Geophys* 34: 531–540
- RŮŽEK B, HRUBCOVÁ P, NOVOTNÝ M, ŠPIČÁK A, KAROUSOVÁ O (2007) Inversion and of travel times obtained during active seismic refraction experiments CELEBRATION 2000, ALP 2002 AND SUDETES 2003. *Stud Geophys Geod* 51: 141–164
- ZELT CA (1994) Software package ZPLOT, Bullard Laboratories. University of Cambridge, Cambridge

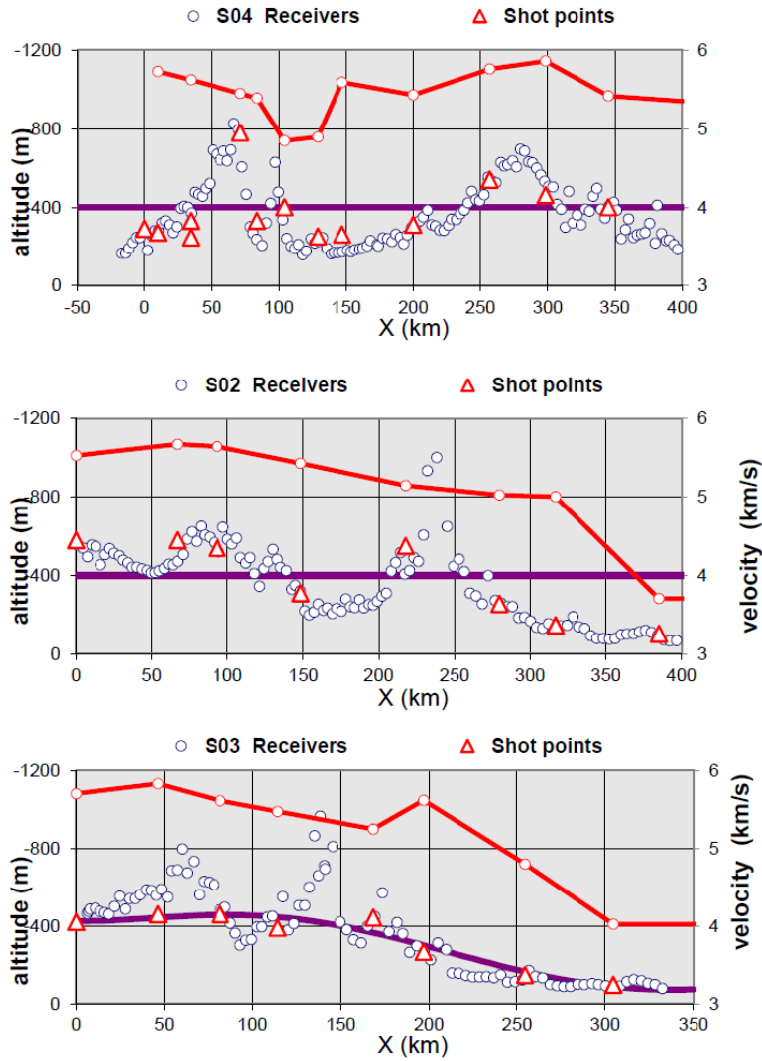


Fig. B1 Altitudes of the S04, S02 and S03 receivers and shot points. Static corrections are computed for the fixed or floating reference levels (bold lines) using the linearly interpolated velocities (red lines) specified at the shot points.

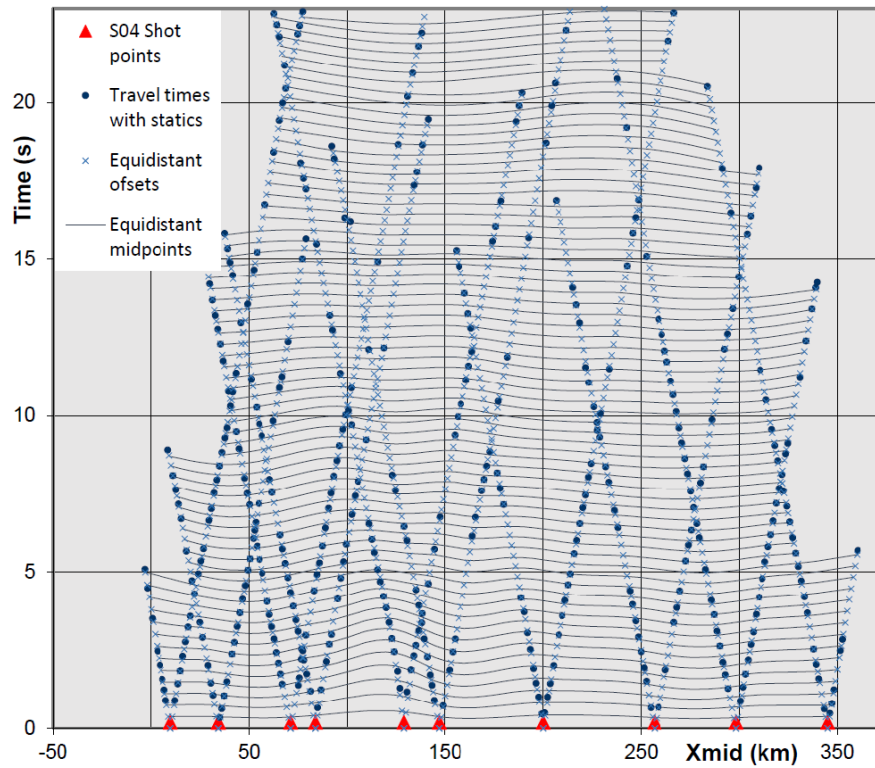


Fig. B2 The refraction arrivals along the S04 profile at their midpoint positions. The maximum offset imaged $q_{\max}=134$ km. ●●● – original picks with introduced static corrections; x x x – travel-times interpolated to the equidistant offsets $q=2, 4, \dots, q_{\max}$; solid lines connect the travel times with fixed offsets interpolated to 5 km midpoint step; ▲ ▲ ▲ – shot-point positions projected to the profile line.

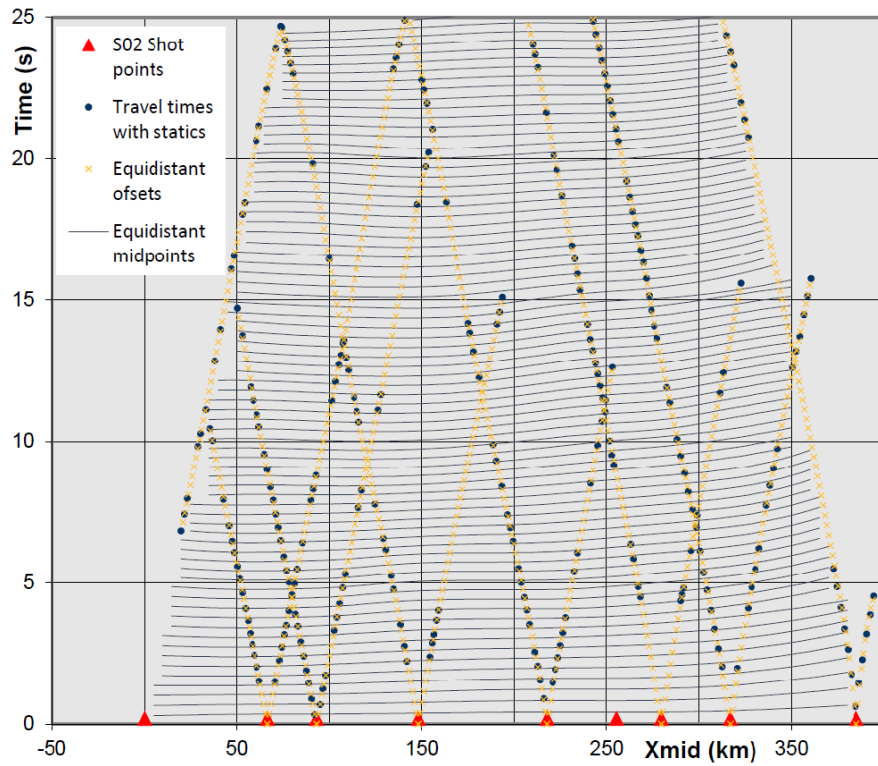


Fig. B2 – continued. The refraction arrivals along the S02 profile at their midpoint positions. The maximum offset $q_{\max} = 146$ km.

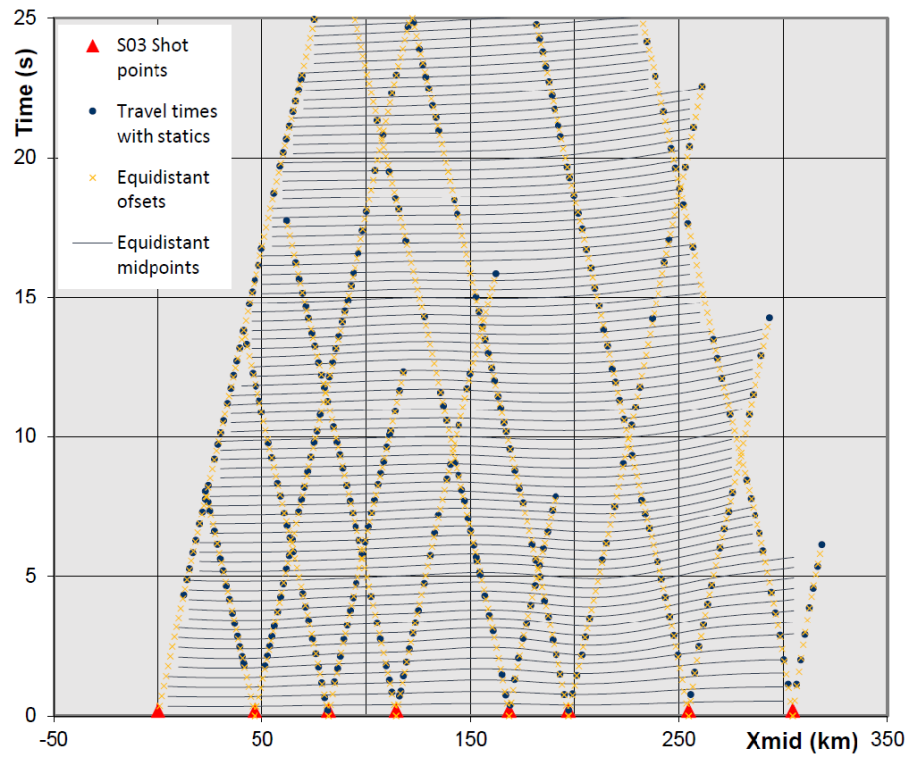


Fig. B2 – continued. The refraction arrivals along the S03 profile at their midpoint positions. The maximum offset $q_{\max} = 148$ km.

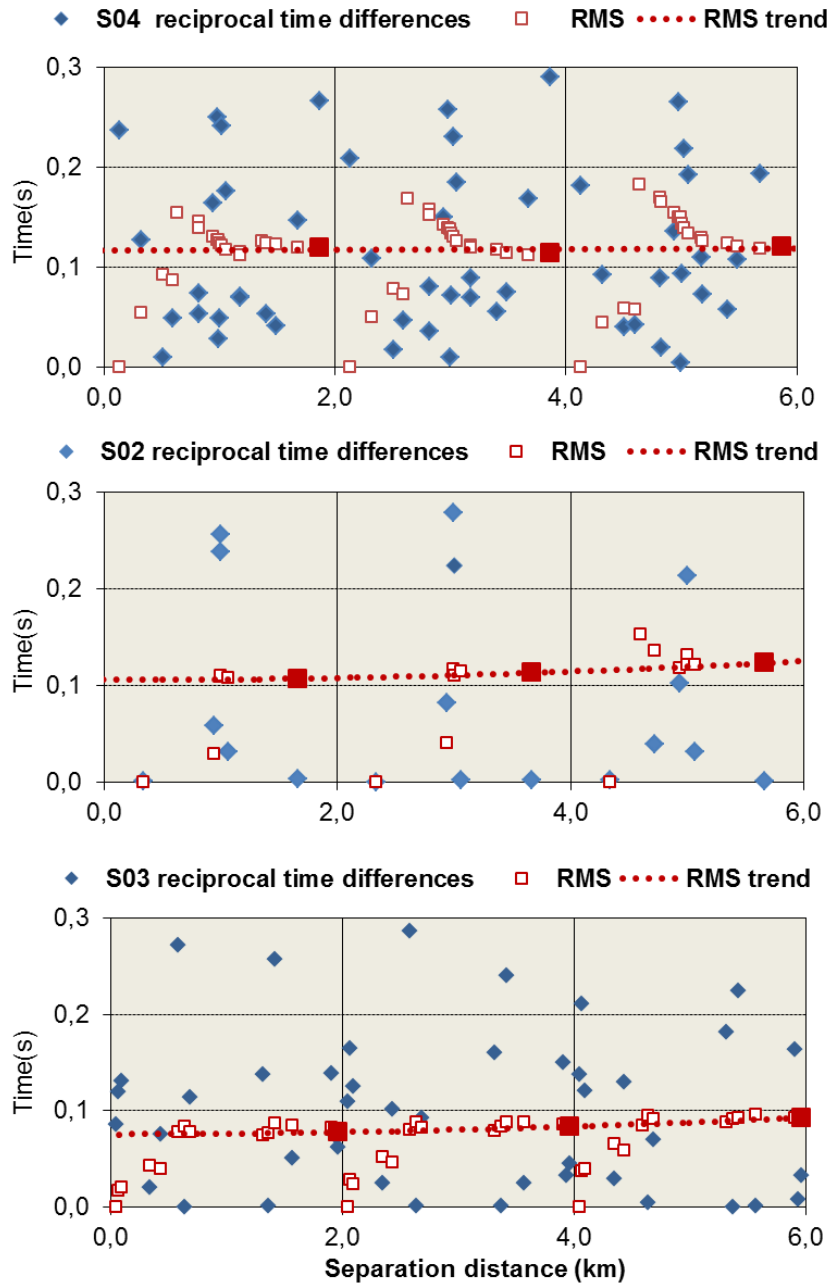


Fig. B3 The differences between the equal-offset travel times (diamonds) near the reciprocal positions on the S04, S02 and S03 profiles. Their RMS are evaluated within three 2-km intervals (open squares) up to the separation distances of 6 km. The total RMS at 2, 4 and 6 km (closed squares) are extrapolated (dotted lines) to yield the proper RMS of reciprocal travel-time discrepancies at the zero separation distance, i.e., 117, 106 and 75 ms, respectively.

Table B1 The shot-point X distances, Y side deviations and Z altitudes along the S04, S02 and S03 profiles derived from the WGS84 coordinates (Grad et al. 2003, Tab. 1)

Line	Shot point	Profile coordinates			Ratio S/N 1-5	Maximum offset (km)	Line	Shot point	Profile coordinates			Ratio S/N 1-5	Maximum offset (km)
		X (km)	Y (km)	Z (m)					X (km)	Y (km)	Z (m)		
S04	44010	0.00	-2.12	-290	4	15	S02	42010	0.00	0.92	-580	3	100
S04	44020	10.04	-6.06	-270	1	200	S02	42020	66.72	-8.05	-580	3	100
S04	44030	34.35	-3.77	-330	1	150	S02	42030	93.06	-0.28	-540	2	120
S04	44031	34.36	-3.86	-245	3	80	S02	44080	148.03	10.09	-310	2	140
S04	44040	71.35	4.80	-780	1	180	S02	42050	217.66	-0.28	-550	3	100
S04	44050	83.86	-6.67	-330	2	110	S02	42070	255.20	-	-440	5	0
S04	41100	104.23	12.10	-400	3	90	S02	41130	279.74	27.15	-256	2	-140, 50
S04	44060	129.04	2.81	-250	3	120	S02	41140	316.74	0.18	-146	1	-300
S04	44070	146.91	-4.32	-260	2	130	S02	42080	384.95	-2.02	-103	1	-300
S04	44080	199.93	1.56	-310	2	130							
S04	44090	256.87	5.95	-540	3	90	S03	43010	0.00	-2.77	-420	1	180
S04	44100	298.28	-1.84	-460	3	-120, 90	S03	44100	46.34	-10.49	-460	1	170
S04	44110	345.10	4.52	-400	2	-140, 90	S03	43020	81.65	1.16	-460	1	140
S04	44140	513.27	14.35	-220	3	-100, 90	S03	43040	114.29	2.20	-390	2	100
S04	44170	598.24	-3.03	-352	2	-120	S03	43060	168.38	-9.90	-442	1	150
S04	44180	610.96	-3.32	-139	2	-130	S03	43070	196.97	-8.27	-266	1	200
S04	44190	624.56	-3.33	-205	3	-60,100	S03	43080	254.54	2.42	-147	1	-200
S04	44210	718.93	-3.52	-88	1	-250	S03	41150	304.47	11.12	-97	1	-200

The positive Y side deviations aim to NE or NW from the S04 or S02, S03 profile lines. The S/N ratios are in the 1-5 scale: 1 indicates the best relative S/N ratio, 5 useless data. The maximum offsets have the negative sign for the readings afore the shots if they are different

Table B2 Assessing the S04, S02 and S03 static corrections referred to the fixed or floating levels (Fig. B2)

Profile S04	Reference level –400 m		
	DTRS	DTR	DTS
max (<i>ms</i>)	35	44	76
min (<i>ms</i>)	–78	–77	–150
σ (<i>ms</i>)	35	30	45
Profile S02	Reference level –400 m		
	DTRS	DTR	DTS
max (<i>ms</i>)	171	91	80
min (<i>ms</i>)	–202	–170	–33
σ (<i>ms</i>)	68	44	43
Profile S03	Floating reference level		
	DTRS	DTR	DTS
max (<i>ms</i>)	91	28	63
min (<i>ms</i>)	–117	–102	23
σ (<i>ms</i>)	35	24	17

The table presents the maxima, minima and standard deviations evaluated for the sets of the partial receiver (DTR), shot-point (DTS) and complete static (DTRS) corrections